THE JOURNAL OF BIOLOGICAL CHEMISTRY VOL. 286, NO. 26, pp. 22924–22933, July 1, 2011

TRAF7 Protein Promotes Lys-29-linked Polyubiquitination of IκB Kinase (IKKγ)/NF-κB Essential Modulator (NEMO) and p65/RelA Protein and Represses NF-κB Activation[S]

Received for publication, December 22, 2010, and in revised form, April 14, 2011 Published, JBC Papers in Press, April 25, 2011, DOI 10.1074/jbc.M110.215426

Tiziana Zotti, Antonio Uva, Angela Ferravante, Mariangela Vessichelli, Ivan Scudiero, Michele Ceccarelli, Pasquale Vito[1], and Romania Stilo

From the Dipartimento di Scienze Biologiche ed Ambientali, Università degli Studi del Sannio, Via Port'Arsa 11, 82100 Benevento and the BioGeM Consortium, Via Camporeale, 83031 Ariano Irpino, Italy

Tumor necrosis factor receptor-associated factor (TRAF) proteins are cytoplasmic regulatory molecules that function as signal transducers for receptors involved in both innate and adaptive humoral immune responses. In this study, we show that TRAF7, the unique noncanonical member of the TRAF family, physically associates with IκB kinase/NF-κB essential modulator (NEMO) and with the RelA/p65 (p65) member of the NF-κB transcription factor family. TRAF7 promotes Lys-29-linked polyubiquitination of NEMO and p65 that results in lysosomal degradation of both proteins and altered activation. TRAF7 also influences p65 nuclear distribution. Microarray expression data are consistent with an inhibitory role for TRAF7 on NF-κB and a positive control of AP-1 transcription factor. Finally, functional data indicate that TRAF7 promotes cell death. Thus, this study identifies TRAF7 as a NEMO- and p65-interacting molecule and brings important information on the ubiquitination events that control NF-κB transcriptional activity.

Tumor necrosis factor receptor-associated factors (TRAFs)[2] have been defined by their ability to couple TNF receptor family proteins to signaling pathways that transduce the cellular effects mediated by TNF family ligands (1, 2). Functionally, TRAF proteins act both as cytoplasmic regulatory molecules and as signal transducers for receptors involved in innate and adaptive humoral immune responses. There are seven known mammalian TRAF proteins (TRAF1–7), of which TRAF1–3 and -5–7 have been shown to interact directly or indirectly with members of the TNF receptor superfamily (1, 2). The domain organization of TRAF proteins is made of a modular structure characteristic of adaptor proteins whose function is to link structurally dissimilar factors. TRAF proteins present a conserved C-terminal coiled-coil domain, the TRAF domain, which is involved in both homo- and heterodimerization (1, 2). Except for TRAF1, TRAFs also contain a conserved RING finger domain and several adjacent zinc finger domains at their N termini (1, 2). The RING finger domains of TRAF2, -6, and -7 have been shown to promote ubiquitination events, which are required for activation of their downstream pathways (3–6).

TRAF7 is the most recently identified member of the family, based on its high homology to the RING and zinc finger domains of TRAF proteins (3, 7). However, TRAF7 lacks the conserved C-terminal domain found in TRAF1–6, and instead it has several WD40 repeats in its C-terminal domain (3, 7). The function of TRAF7 is still not completely elucidated. TRAF7 specifically interacts with MEKK3 and potentiates MEKK3-mediated signaling (3, 7). TRAF7 also binds to c-Myb and stimulates its sumoylation, thereby inhibiting its trans-activation activity (8). Finally, it has been shown that TRAF7 is involved in the signal transduction pathway that links Toll-like receptor 2 stimulation to activation of NF-κB transcription factor (9). In fact, among the TRAF family of proteins, TRAF2, -5, and -6 are activators of the canonical NF-κB pathway, which involves activation of the IκB kinase complex, leading to the degradation of IκBα, nuclear translocation of the predominant p50/p65 transcription complex, and activation of genes with pleiotropic roles in cell survival and immune and inflammatory responses (10, 11). In an effort to discover proteins that interact with NEMO, we carried out a yeast two-hybrid screen that identified TRAF7 as a NEMO-interacting protein. Here, we report a negative role for TRAF7 in NF-κB signaling.

EXPERIMENTAL PROCEDURES

Two-hybrid Screening—The two-hybrid screening was performed using the Matchmaker system (Clontech) as described previously (12). Briefly, yeast strain AH109 GAL4$^{-/-}$ was first transformed with pGBKT7 plasmids carrying a cDNA bait fused with DNA binding domain of GAL4 using the lithium acetate/PEG3000 procedure. Transformant colonies were selected on synthetic dropout plates lacking tryptophan. Expression of bait fusion proteins was assessed by immunoblot analysis. For library screening, yeast AH109 expressing GAL4DBD-NEMO(1–339) was transformed with a human cDNA library cloned in pACT2 vector (Clontech) in fusion with GAL4TAD. 2×10^6 clones were screened for interaction with GAL4DBD-NEMO(1–339) using selective growth on minimal medium lacking nutrients whose biosynthesis is mediated by genes under control of GAL4 transcriptional activity.

Cell Culture, Plasmids, and Antibodies—HEK293 and HeLa cells were cultured in Dulbecco's modified Eagle's medium supplemented with 10% FCS and transfected by calcium phosphate

[S] The on-line version of this article (available at http://www.jbc.org) contains supplemental data S1 and S2.

[1] To whom correspondence should be addressed. E-mail: vito@unisannio.it.

[2] The abbreviations used are: TRAF, tumor necrosis factor receptor-associated factor; MTT, 3-(4,5-dimethylthiazol-2-yl)-2,5-diphenyltetrazolium bromide; LPA, lysophosphatidic acid; NEMO, NF-κB essential modulator.

precipitation. Lentiviral vectors expressing shTRAF7 RNAs were obtained from Sigma and used according to the manufacturer's instructions. Plasmids encoding mutant ubiquitins were a kind gift of Dr. C. Sasakawa, University of Tokyo.

Sources of antisera and monoclonal antibodies were as follows: anti-TRAF7, Imgenex; anti-FLAG and anti-β-actin, Sigma; anti-NEMO, anti-HA, anti-p65, anti-ubiquitin (P4D1), anti-β tubulin, and anti-acetyl-histone H3, Santa Cruz Biotechnology. TNFα, IL1β, LPS, MG132, LPA, leupeptin, phorbol 12-myristate 13-acetate, ionomycin, and cycloheximide were from Sigma.

Immunoblot Analysis and Coprecipitation—Cell lysates were made in lysis buffer (150 mM NaCl, 20 mM Hepes, pH 7.4, 1% Triton X-100, 10% glycerol, and a mixture of protease inhibitors). Proteins were separated by SDS-PAGE, transferred onto nitrocellulose membrane, and incubated with primary antibodies followed by horseradish peroxidase-conjugated secondary antibodies (Amersham Biosciences). Blots were developed using the ECL system (Amersham Biosciences). For coimmunoprecipitation experiments, cells were lysed in lysis buffer, and immunocomplexes were bound to protein A/G (Roche Applied Science), resolved by SDS-PAGE, and analyzed by immunoblot assay.

GST Pulldown Assay—To analyze NEMO interaction with TRAF7, NEMO-glutathione *S*-transferase (GST) fusion protein was generated in *Escherichia coli* DH5α cells using pGEX-5x-1 as plasmid (GE Healthcare). Transformed bacteria were grown at 37 °C until an A_{600} of 0.6 and induced with 1 mM isopropyl 1-thio-β-D-galactopyranoside for 3 h at 37 °C. NEMO-GST fusion protein expression was assessed by SDS-PAGE. Cells were lysed with five freeze-thaw cycles followed by 1 min of sonication. After centrifugation, soluble fraction was bound to glutathione-Sepharose beads (GE Healthcare) in an EconoPac chromatography column (Bio-Rad) overnight at 4 °C on a rotating wheel. Beads were then washed twice with PBS and resuspended in lysis buffer with protease inhibitors (Roche Applied Science). Lysates obtained from HEK293 cells were mixed with Sepharose-bound GST-NEMO (2 μg) overnight at 4 °C on a rotating wheel. Beads were spun down, washed three times with lysis buffer without protease inhibitors, and resuspended in Laemmli Buffer. Samples were boiled for 5 min, and supernatants were separated by SDS-PAGE followed by blotting and incubation with TRAF7 antibody.

Luciferase Assay—To assess NF-κB and AP-1 activation, HEK293 cells were transfected with the indicated plasmidic DNAs together with pNF-κB-luc or pAP-1-luc (Clontech) in 6-well plates. Silenced HeLa cells were transfected with Attractene reagent (Qiagen) following the manufacturer's protocol. 24 h after transfection, luciferase activity was determined with Luciferase assay system (Promega). Plasmids expressing RSV-β-galactosidase or TK-*Renilla* were used in transfection mixtures to normalize efficiency of transfection.

Immunofluorescence—HEK293 and HeLa cells were grown and transfected in chamber slides. 24 h later, cells were fixed in 3% paraformaldehyde for 10 min at room temperature and then permeabilized in 0.2% Triton X-100 for 5 min. Cells were incubated for 1 h with primary antibodies in PBS followed by three washes with PBS and a second incubation with FITC-conjugated secondary antibody for 1 h. After three washes with PBS, nuclei were stained with DAPI for 5 min. Chamber slides were dried and analyzed with fluorescence microscopy. All steps were done at room temperature.

TABLE 1

Yeast AH109 was transformed with TRAF7(266–670) fused to the GAL4-TAD together with the indicated cDNAs fused to GAL4-DBD

The cDNA encoding for FADD served as a negative control. The interactions were examined by yeast growth on selective media; assays were done for 5–10 independent transformants. Yeast colonies were scored as positive when a growth developed within 24–36 h; a negative was scored when growth failed to develop within 1 week.

Interaction of NEMO with TRAF7 in the yeast two-hybrid assay		
Protein fused to GAL4 domain		Yeast growth on selective media
DNA binding	Activating	
	TRAF7(266–670)	−
Vector	TRAF7(266–670)	−
FADD	TRAF7(266–670)	−
NEMO(1–339)	TRAF7(266–670)	+

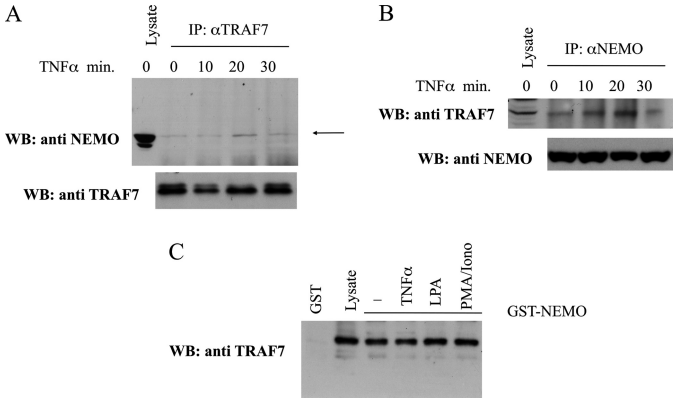

FIGURE 1. **TRAF7 binds to NEMO.** *A*, HEK293 cells were treated with TNFα (10 ng/ml) for the indicated periods of time. Cell lysates were immunoprecipitated (*IP*) with anti-TRAF7 antibody and analyzed by immunoblot probed with anti-NEMO. *WB*, Western blot. *B*, HEK293 cells were treated as in *A*. Cell lysates were immunoprecipitated with anti-NEMO and probed with anti-TRAF7 antibody. *C*, cell lysates were prepared from HEK293 cells left untreated or stimulated for 20 min (TNFα, 10 ng/ml; LPA, 10 μM; phorbol 12-myristate 13-acetate, 40 ng/ml plus ionomycin 1 μM) and incubated with Sepharose-GST-NEMO or GST alone. Pulled down proteins were probed with anti-TRAF7 antibodies. Autoradiographs shown are representative of four independent experiments.

RNA Microarray—Single strand biotinylated cDNA was generated as follows; 100 ng of total RNA were subjected to two cycles of cDNA synthesis with the Ambion WT expression kit (Applera). The first cycle was performed using an engineered set of random primers that excludes rRNA-matching sequences and includes the T7 promoter sequence. After second strand synthesis, the resulting cDNA was transcribed *in vitro* with the T7 RNA polymerase to generate a cRNA. This cRNA was subjected to a second cycle-first strand synthesis in the presence of dUTP in a fixed ratio relative to dTTP. Single strand cDNA was then purified and fragmented with a mixture of uracil DNA glycosylase and apurinic/apyrimidinic endonuclease 1 (Affymetrix) that break the DNA strand specifically at the unnatural dUTP residues. DNA fragments were then terminally labeled by terminal deoxynucleotidyltransferase (Affymetrix) with biotin. The biotinylated DNA was hybridized to the Human GeneChip Gene 1st Arrays (Affymetrix), containing almost 29,000 genes selected from *Homo sapiens* genome databases RefSeq, ENSEMBL, and GenBank™. Chips

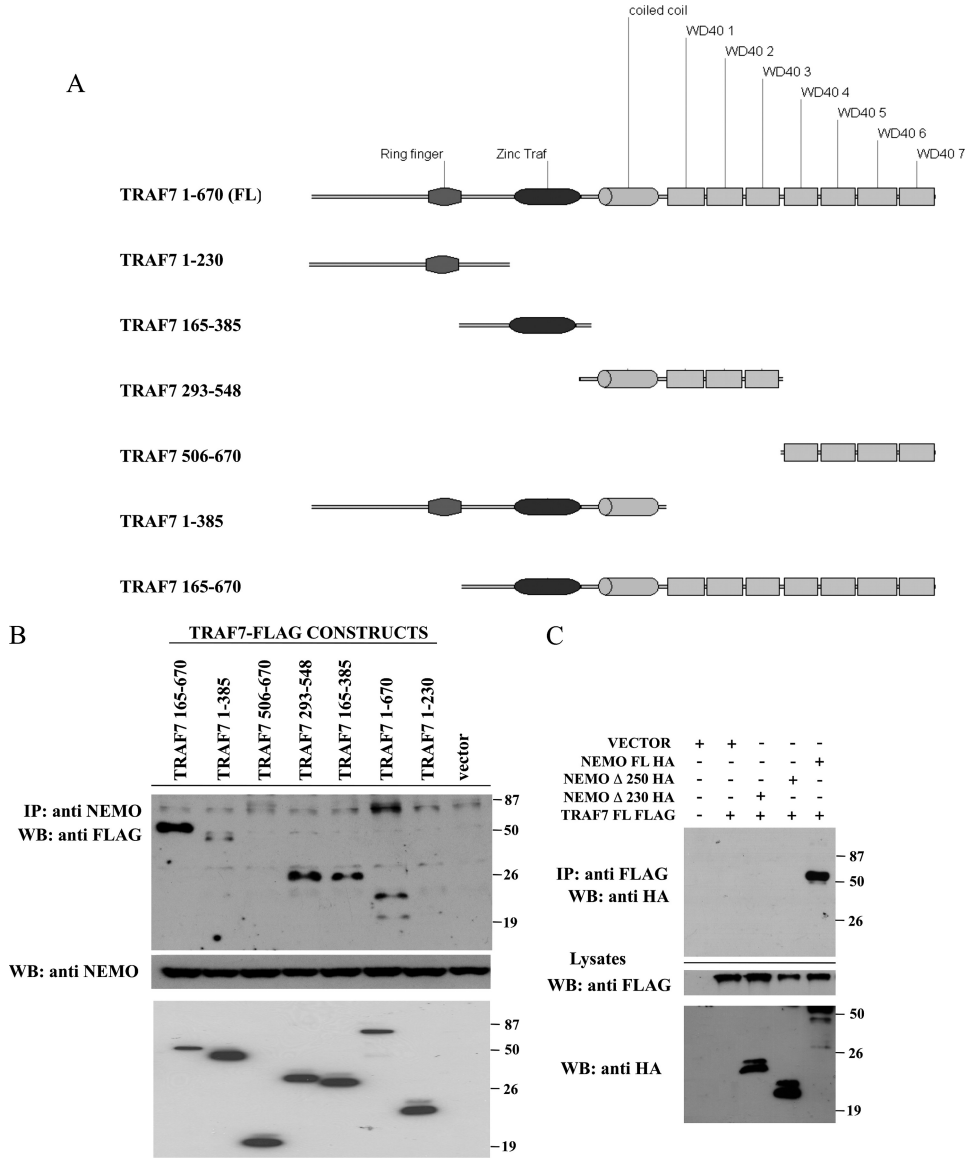

FIGURE 2. **Mapping of the regions involved in the association of TRAF7 with NEMO.** *A,* schematic representation of the TRAF7 constructs used in this study. *B,* HEK293 cells were transfected with a vector expressing the indicated FLAG-tagged TRAF7 polypeptides. 24 h later, cell lysates were immunoprecipitated (*IP*) with anti-NEMO antibody and analyzed by immunoblot probed with anti-FLAG mAb. *WB*, Western blot. *C,* HEK293 cells were transfected with a vector expressing the indicated FLAG- and HA-tagged polypeptides. 24 h later, cell lysates were immunoprecipitated with anti-HA and analyzed by immunoblot probed with anti-FLAG mAb.

were washed and scanned on the Affymetrix Complete GeneChip Instrument System, generating digitized image data files.

Microarray Data Analysis—Digitized image data files were analyzed by expression console (Affymetrix Inc.). The full data set was normalized by using the Robust Multialignment Algorithm. The expression values obtained were analyzed by using GeneSpring 10.3 (Agilent Technologies). Further normalization steps included a per chip normalization to the 50th percentile and a per gene normalization to the median. Results were filtered for fold change of >1.4. Statistical analysis was performed using analysis of variance, using a p value cutoff of 0.05.

Real Time—Real time PCRs were performed in triplicate (primer sequences are detailed in supplemental data S2) by using the SYBR Green PCR master mix (Qiagen) in a 7900HT sequence detection system (Applied Biosystems). The relative transcription level was calculated by using the $\Delta\Delta Ct$ method.

Subcellular Fractionation—HEK293 cells were washed twice with PBS, scraped, and lysed in lysis buffer (0,5% Nonidet P-40, 50 mM KCl, 100 μM DTT, 1 mM PMSF, and an antiprotease mixture). After centrifugation, the supernatant was used as a cytoplasmic fraction. The pellet was first washed three times with washing buffer (25 mM Hepes, pH 7.8, 50 mM KCl, 100 μM DTT, 1 mM PMSF, and antiprotease) and then extracted with Nuclear Extraction Buffer (25 mM Hepes, pH 7.8, 500 mM KCl, 10% glycerol, 100 μM DTT, 1 mM PMSF, and antiprotease). After centrifugation, the supernatant was used as nuclear fraction. All steps were done at 4 °C.

MTT Assay—At the end of each testing time, the culture supernatants were removed, and MTT solution (0.5 mg/ml)

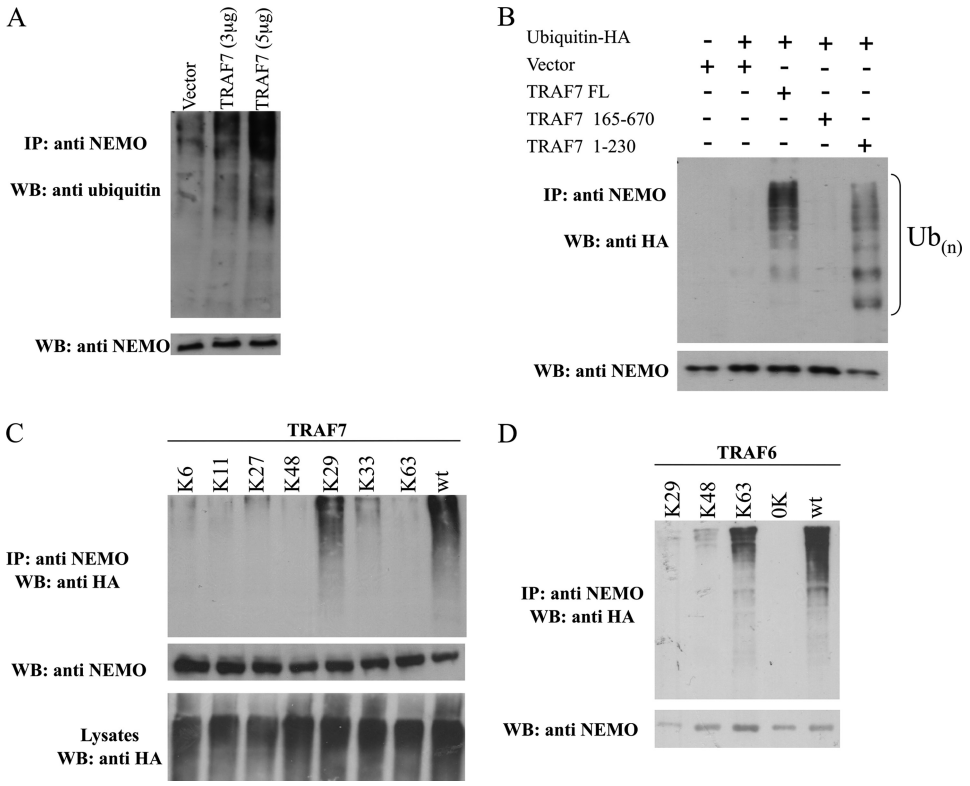

FIGURE 3. **TRAF7 promotes ubiquitination of NEMO.** *A,* HEK293 cells were transfected with the indicated amount of a vector expressing TRAF7. 24 h later, cell lysates were immunoprecipitated (*IP*) with anti-NEMO antibody, separated by SDS-PAGE, and transferred onto membranes subsequently probed with anti-ubiquitin. *WB*, Western blot. *B,* HEK293 cells were cotransfected with the indicated constructs; cell lysates were immunoprecipitated with anti-NEMO antibody and analyzed by immunoblot probed with anti-HA. *C,* HEK293 cells were cotransfected with FLAG-tagged TRAF7 and HA-tagged ubiquitin (*Ub*) mutants; the number (*n*) indicates the only lysine residue remaining in the ubiquitin molecule. Immunoprecipitates with anti-NEMO antibody were resolved by SDS-PAGE and blotted onto a membrane subsequently probed with anti-HA. A fraction of cell lysates was probed with anti-HA antibody to monitor expression and usage of all ubiquitin mutants. *D,* HEK293 cells were cotransfected with TRAF6 and HA-tagged ubiquitin mutants as in *C*, and anti-NEMO immunoprecipitates were analyzed by immunoblot probed with anti-HA.

was added to each well, and the plates were incubated for 1 h at 37 °C. The MTT solution was removed, and isopropyl alcohol was added to dissolve formazan crystals. The absorbance at 570 nm was read on a microplate spectrophotometer (Applied Biosystem). The percentage of viability was calculated as $(AT/AC) \times 100$, where AT and AC are the absorbance of treated and control cells, respectively.

RESULTS

By using a yeast two-hybrid-based screening assay with NEMO(1–339) as a bait and a target human fetal brain cDNA library, we identified a total of 20 NEMO-positive unique interacting clones. One of them encoded a portion of TRAF7 spanning amino acidic residues 266–670 (TRAF(266–670)), thus consisting of a polypeptide containing a portion of the zinc finger domain, the coiled-coil domain, and the seven WD40 repeats. When tested in a bait/interactor format, NEMO was shown to interact with TRAF(266–670) in yeast (Table 1).

To verify association of TRAF7 with NEMO in mammalian cells, lysates from HEK293 cells were immunoprecipitated with anti-TRAF7, and coprecipitating proteins were analyzed for the presence of NEMO by the immunoblotting assay. As shown in Fig. 1*A*, immunoprecipitation of endogenous TRAF7 revealed association with NEMO in HEK293 cell lysates. In the reciprocal experiment, immunoprecipitation of endogenous NEMO revealed the presence of coprecipitated TRAF7 (Fig. 1*B*). In both experiments, cell stimulation with TNFα induced TRAF7/NEMO interaction, which peaked at 20 min following stimulation (Fig. 1, *A* and *B*). Based on pulldown assays, GST-fused recombinant NEMO bound to the endogenous TRAF7 in HEK293 cell extracts (Fig. 1*C*). No pulldown was detectable using GST alone, indicating that NEMO specifically binds TRAF7 *in vitro* as well as in intact mammalian cells. In this experimental system, cellular stimulation with TNFα, LPA, and phorbol 12-myristate 13-acetate/ionomycin did not increase association of recombinant NEMO with endogenous TRAF7 (Fig. 1*C*). Overall, this set of experiments demonstrates that there is a physical interaction between NEMO and TRAF7, which is induced, *in vivo*, by TNFα stimulation.

To define the region of TRAF7 involved in the association with NEMO, HEK293 cells were cotransfected with plasmids expressing FLAG-tagged TRAF7 polypeptides (Fig. 2*A*). Cell lysates were immunoprecipitated for endogenous NEMO, and the presence of coprecipitating TRAF7 polypeptides was assessed by immunoblots probed with anti-FLAG antibody. The results of these experiments, shown in Fig. 2*B*, indicated that in mammalian cells TRAF7(1–670), TRAF7(165–385), TRAF7(293–548), TRAF7(1–385a0, and TRAF7(165–670) associated with NEMO, whereas TRAF7(1–230) and TRAF7 (506–670) did not. Collectively, these experiments indicated

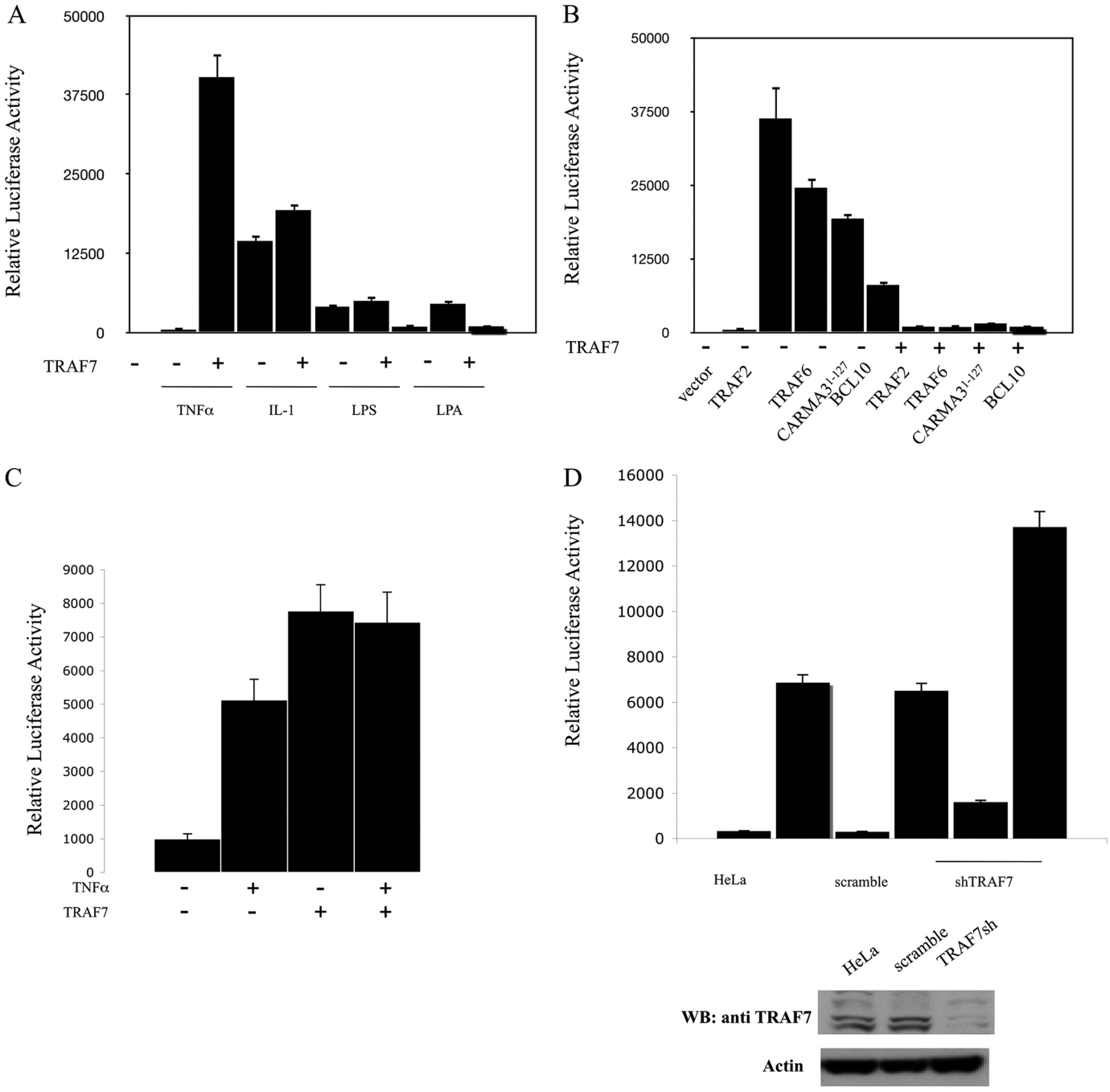

FIGURE 4. **Inhibition of NF-κB activation by TRAF7.** *A,* HEK293 cells were transfected with pNF-κB-luciferase plasmid, a β-galactosidase reporter vector, and an expression vector encoding for TRAF7, where indicated. 24 h later, cells were treated with the indicated stimuli (TNFα, 10 ng/ml; IL-1β, 20 ng/ml; LPS, 1 μg/ml; LPA, 10 μM) for 4 h. Data shown represent the relative luciferase activity normalized against β-galactosidase activity and are representative of at least 10 independent experiments performed in triplicate. *B,* HEK293 cells were transiently cotransfected with an expression vector encoding the indicated polypeptides, together with NF-κB-luciferase and β-galactosidase reporter vectors. The total amount of transfected plasmidic DNA was maintained constant by adding empty vector. 24 h after transfection, cell lysates were prepared and luciferase activity was measured. Data shown represent relative luciferase activity normalized against β-galactosidase activity and are representative of at least 10 independent experiments performed in triplicate. *C,* HEK293 cells were transfected with an AP-1-luciferase reporter plasmid and an expression vector encoding for TRAF7 and stimulated with TNFα (10 ng/ml) for 6 h where indicated. Reporter gene assay was performed as in *A* and *B*. *D,* HeLa cells were left untreated or infected with lentiviral vectors encoding for shRNAs for human TRAF7 or a control sequence (see supplemental data S2). After selection of infected cells, the expression level of TRAF7 was monitored by Western blot (*WB*) experiments (*right panel*). Cells were then transfected with pNF-κB-luciferase plasmid and 24 h later treated with TNFα (10 ng/ml) for 4 h. Cell lysates were then prepared, and luciferase activity was measured. Data shown represent relative luciferase activity normalized on β-galactosidase activity and are representative of six independent experiments done in triplicate.

that the coiled-coil domain of TRAF7 is required for association with NEMO. Similar experiments performed using deletion mutants of NEMO indicated that residues 1–230 of NEMO are required for binding to TRAF7 (Fig. 2*C*).

Recently, we and others have shown that ubiquitination events play a key role in regulating the function of NEMO (4, 13). Therefore, we examined whether TRAF7 was able to influence the ubiquitination state of NEMO. For this, we transfected

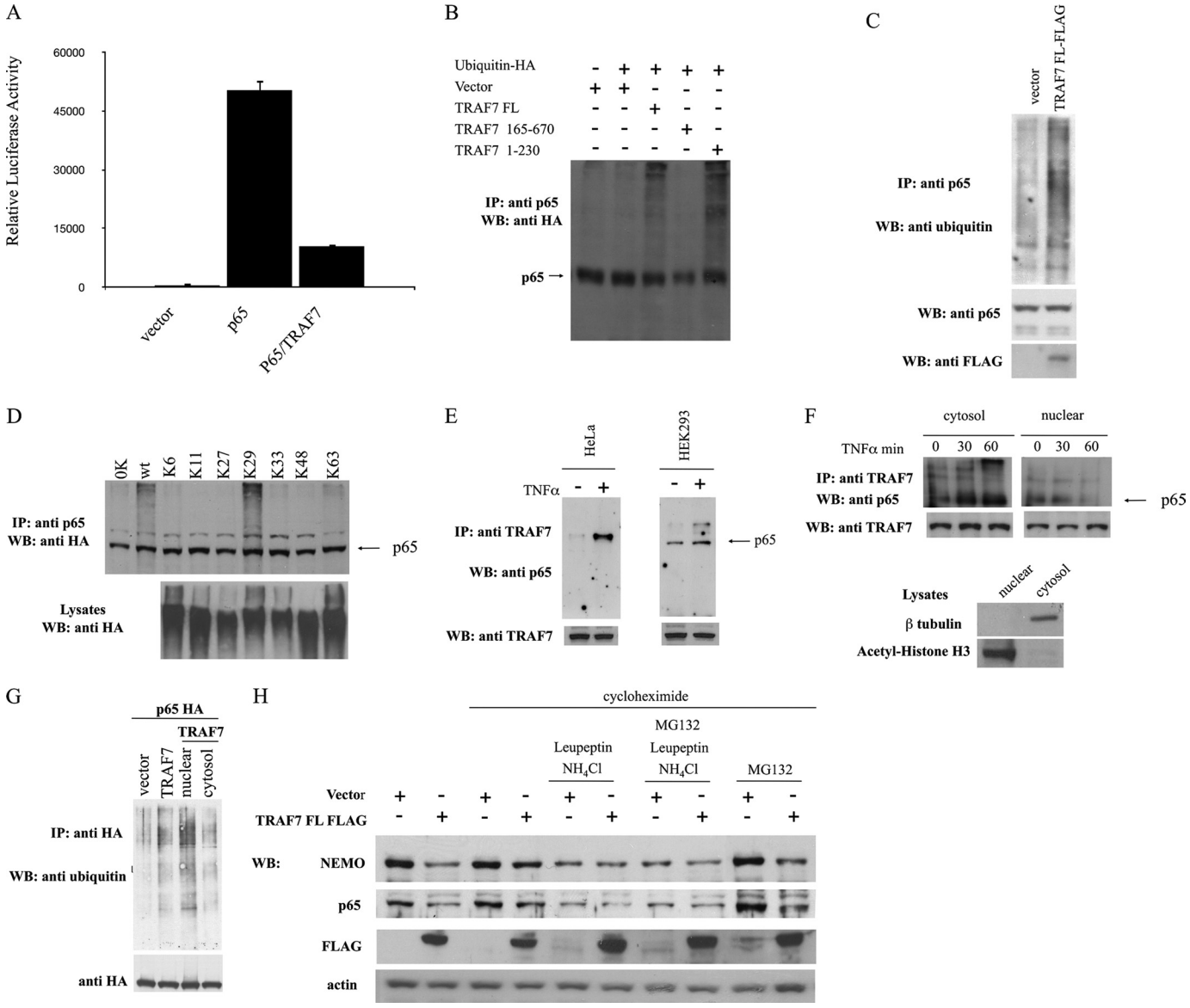

FIGURE 5. **TRAF7 inhibits p65 transcriptional activity.** *A,* HEK293 cells were transiently cotransfected with an expression vector encoding for the p65 subunit of NF-κB, together with pNF-κB-luciferase and β-galactosidase reporter vectors. 24 h after transfection, cell lysates were prepared, and luciferase activity was measured. Data shown represent the relative luciferase activity normalized against β-galactosidase activity and are representative of at least 10 independent experiments performed in triplicate. *B,* HEK293 cells were transfected with the indicated constructs; cell lysates were immunoprecipitated (*IP*) with anti-p65 antibody and analyzed by immunoblot with anti-HA and anti-p65. *C,* HEK293 cells were transfected with a vector empty or encoding for TRAF7. 24 h later, cell lysates were immunoprecipitated with anti-p65 antibody and analyzed by immunoblot probed with anti-ubiquitin antibody (P4D1). *D,* HEK293 were transfected with a vector expressing TRAF7 along with HA-tagged mutated ubiquitins. 24 h later, cell lysates were immunoprecipitated (*IP*) with anti-p65 antibody and analyzed by immunoblot probed with anti-HA followed by anti-p65. A fraction of cell lysates was probed with anti-HA antibody to monitor expression and usage of ubiquitin mutants used. *WB*, Western blot. *E,* HEK293 and HeLa cells were treated with TNFα (10 ng/ml) for 30 min. Cell lysates were immunoprecipitated with anti-TRAF7 and subsequently hybridized with anti-p65. *F,* HEK293 cells were treated with TNFα (10 ng/ml) for 30 min, and nuclear and cytosolic extracts were prepared. Lysates were then immunoprecipitated with anti-TRAF7 and tested for p65 by immunoblot experiments. *G,* total and fractionated lysates of HEK293 cells transfected with p65-HA and TRAF7 were immunoprecipitated with anti-HA, and analyzed by immunoblot probed with anti-ubiquitin. *H,* HEK293 cells were transfected with an expression vector empty or encoding for TRAF7. Cells were left untreated or treated with lysosomal (leupeptin 50 μM + NH_4Cl 10 mM) or proteasomal (MG132 10 μM) inhibitors for 3 h and analyzed by immunoblot assay.

HEK293 cells with TRAF7 and assessed the ubiquitination state of NEMO by immunoblot experiments. As shown in Fig. 3*A*, TRAF7 promoted endogenous ubiquitination of NEMO in a dose-dependent manner. The NEMO ubiquitinating activity was retained in a TRAF7 deletion mutant that contains the ring finger domain, which was lost in a TRAF7 deletion mutant that lacks that domain (Fig. 3*B*). As ubiquitin possesses seven lysines (Lys-6, Lys-11, Lys-27, Lys-29, Lys-33, Lys-48, and Lys-63) and the fate of ubiquitinated proteins depends on the Lys-type of linkage, we used a series of ubiquitin mutants possessing single lysine residues to investigate the nature of TRAF7-mediated ubiquitination of NEMO. NEMO was only ubiquitinated by the Lys-29-Ub (K29-Ub) mutant to a similar extent as by wild-type ubiquitin (Fig. 3*C*). In the same experimental condition, TRAF6 promoted Lys-63 ubiquitination of NEMO (Fig. 3*D*), thus validating the specificity of Lys-29-ubiquitination mediated by TRAF7.

As ubiquitination of NEMO regulates activation of the IκB kinase complex (4), we tested whether expression of TRAF7

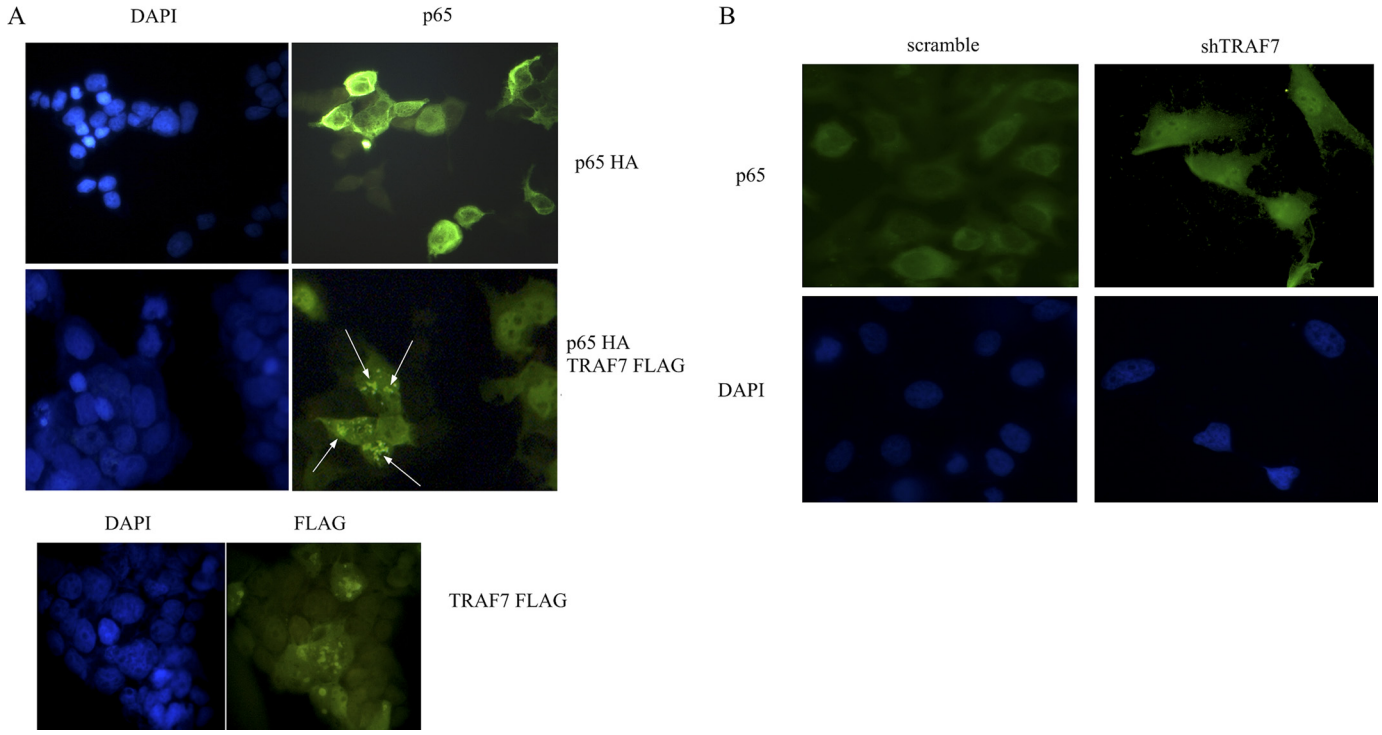

FIGURE 6. **Fluorescence micrographs of p65.** *A,* HEK293 cells expressing p65 alone or in the presence of an excess of TRAF7 were stained with anti-p65Ab followed by FITC-conjugated anti-mouse IgG. *B,* HeLa cells expressing an shRNA targeting TRAF7 or a control shRNA were stained with anti-p65Ab followed by FITC-conjugated anti-goat IgG.

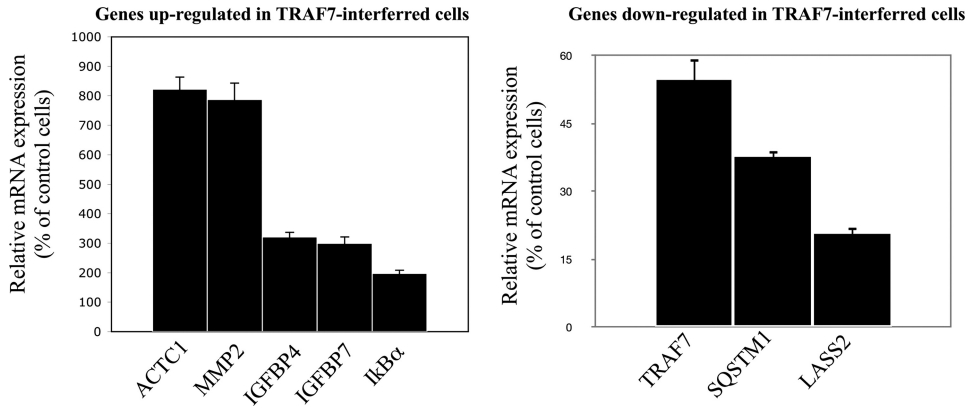

FIGURE 7. **Real time PCR quantitation of mRNA levels of selected genes normalized to GAPDH in HeLa cells silenced with TRAF7 shRNA.** Oligonucleotides used for real time PCR quantitation are detailed in supplemental data S2.

modulates activation of the NF-κB transcription factor using an NF-κB-luciferase reporter assay. In all the experimental conditions tested, TRAF7 was unable to activate NF-κB (data not shown). However, we noted that TRAF7 expression dramatically reduces NF-κB activation induced by either exogenous stimuli, such as TNFα, IL-1β, LPS, and LPA treatments, or by transfection of expression vectors encoding for well known activators of NF-κB (Fig. 4, *A* and *B*).

In the same experimental system, TRAF7 expression induced AP-1 activity at least 9–10-fold compared with empty vector, which is higher than the AP-1 activity elicited by TNFα stimulation (Fig. 4*C*). We also measured the effect of shRNA-mediated knockdown of TRAF7 on the expression of an NF-κB-driven luciferase reporter construct. For this, we used a lentiviral expression vector encoding a short hairpin RNA (shRNA) designed to target human TRAF7 for degradation by the RNAi pathway. Lentivirus infection of HeLa cells resulted in reduced TRAF7 protein expression (Fig. 4*D*). When assayed in the NF-κB-luciferase reporter tests, this construct produced a higher NF-κB-driven luciferase activity (Fig. 4*D*). Similar results were obtained when HEK293 cells were used for these experiments (data not shown).

Inhibition of NF-κB activation in HEK293 cells expressing TRAF7 was also assessed by monitoring degradation of the inhibitory subunit I-κBα following TNFα stimulation. Immunoblot assays indicate that TRAF7 partially suppresses degradation of the inhibitory subunit I-κBα and delays p65 entry into the nucleus following TNFα treatment (supplemental data S1). Overall, these experiments indicated that TRAF7 acts as a negative regulator of NF-κB and functions as a positive regulator of AP-1.

Surprisingly, TRAF7 expression also inhibited activation of NF-κB induced by transfection of a plasmid encoding for the

p65 subunit of NF-κB (Fig. 5*A*). This observation prompted us to investigate whether TRAF7 expression alters the ubiquitination state of p65, thereby influencing its transcriptional activity. For this, we transfected HEK293 cells with exogenous HA-tagged ubiquitin and assessed the ubiquitination state of endogenous p65 by immunoblot experiments. As shown in Fig. 5*B*, TRAF7 promoted ubiquitination on p65. The same result was obtained when we monitored both p65 and ubiquitin endogenous proteins (Fig. 5*C*). Also, experiments done using mutated ubiquitins indicated that, similarly to NEMO, TRAF7 promotes Lys-29-linked ubiquitination of p65 (Fig. 5*D*).

It is well known that a variety of coregulators influence NF-κB signaling, and most of these can physically associate with NF-κB family proteins (14). Thus, we tested whether TRAF7 can physically bind to p65. Immunoprecipitation of endogenous TRAF7 revealed a strong association with endogenous p65 in HeLa and HEK293 cells upon TNFα stimulation (Fig. 5*E*). In addition, cell fractionation experiments revealed that, following TNFα stimulation, the cytoplasmic levels of p65 and TRAF7 association increase, whereas the nuclear association follows an opposite kinetic (Fig. 5*F*). In similar fractionation experiments, p65 appears ubiquitinated by TRAF7 in both cytosolic and nuclear compartments (Fig. 5*G*).

As Lys-29 ubiquitination has been linked to lysosomal degradation (20), we monitored the expression levels of endogenous NEMO and p65 in the presence of TRAF7 in cells untreated or treated with lysosomal (leupeptin + NH_4Cl) or proteasomal (MG132) inhibitors. In untreated cells, TRAF7 expression lowered the protein levels of both NEMO and p65 (Fig. 5*H*, *1st* and *2nd lanes*). Treatment with MG132 does not restore NEMO and p65 expression (Fig. 5*H*, *9th* and *10th lanes*), thus excluding the possibility of a TRAF7-mediated proteasomal degradation of these proteins. However, in cells exposed to the lysosomal inhibitors, the expression levels of NEMO and p65 are not significantly different in cells transfected with empty vector or TRAF7 (Fig. 5*H*, *5th* to *8th lanes*).

We next tested whether TRAF7 influences the cellular distribution of p65. For this, we transfected HEK293 cells with a vector encoding for p65, either alone or in the presence of an excess of TRAF7, and determined the cellular localization of p65. The results in Fig. 6*A* show that whereas p65 alone exhibits a uniform pattern of cytosolic and nuclear distribution, in the presence of TRAF7 it localizes in discrete and punctate nuclear structures. We also determined the localization of endogenous p65 in HeLa cells expressing a shRNA targeting TRAF7 or expressing a scramble shRNA. These experiments, shown in Fig. 6*B*, indicate that TRAF7 knockdown results in increased nuclear localization of endogenous p65 in unstimulated cells.

To assess the role of TRAF7 in global transcriptome, finally we compared TRAF7-silenced *versus* nonspecific siRNA-infected cells on Affymetrix microarrays. Analysis was conducted in triplicate, and significant gene expression variation was considered for a fold change ≥1.4, corresponding to the average reduction of TRAF7 gene expression in silenced cells. Data analysis identified 55 varying genes, of which 14 were up-regulated (25.4%) and 41 were down-regulated (74.6%) in silenced cells with respect to control cells. A selection of these genes was confirmed by real time PCR (Fig. 7 and data not shown). Genes up-regulated in TRAF7-silenced cells included the NF-κB regulated gene serine protease inhibitor serpin2E and the insulin-like growth factor binding protein-4 and -7, and α-synuclein (Table 2). Among genes down-regulated in TRAF7-silenced cells, there are several stress-related genes, and cell cycle-related genes (Table 3).

Because NF-κB transcription factor has a beneficial effect on cell survival and proliferation, we predicted that expression of

TABLE 2
Up-regulated genes in TRAF7-silenced cells

	iTRAF7 *versus* WT		
	Up-regulated genes		
	Cluster ID	Gene symbol	GenBank™
1	7919627	*HIST2H4A*	BC108260
2	7931097	*HTRA1*	D87258
3	7975390	*SMOC1*	AK289988
4	7987315	*ACTC1*	BC009978
5	7991335	*ANPEP*	BC058928
6	7995681	*MMP2*	BC002576
7	8007100	*IGFBP4*	BC016041
8	8035829	*RPL34|LOC342994*	CR542242
9	8056860	*WIPF1*	BX640870
10	8059376	*SERPINE2*	BC042628
11	8100541	*IGFBP7*	BC017201
12	8101762	*SNCA*	BC108275
13	8134257	*GNG11*	BC009709
14	8141016	*TFPI2*	AK129833

TABLE 3
Down-regulated genes in TRAF7-silenced cells

	iTRAF7 *versus* WT		
	Down-regulated genes		
	Cluster ID	Gene symbol	Genbank™
1	7898693	*ALPL*	BC090861
2	7919856	*LASS2*	BC001357
3	7925929	*AKR1C3*	BC001479
4	7927964	*SRGN*	BC015516
5	7931832	*AKR1C2*	BC063574
6	7942123	*CCND1*	BC023620
7	7942957	*PRSS23*	BC001278
8	7948229	*SLC43A3*	AB028927
9	7953291	*CD9*	AY966455
10	7956076	*CDK2*	BC003065
11	7960340	*FOXM1*	U74612
12	7960933	*M6PR*	BC024206
13	7983650	*SLC27A2*	D88308
14	7992529	*TRAF7*	AY569455
15	8005475	*TRIM16L*	DQ232882|AK056026
16	8018975	*LGALS3BP*	L13210
17	8025672	*SLC44A2*	BC040556
18	8034940	*NOTCH3*	U97669
19	8049670	*GPC1*	X54232
20	8065637	*COMMD7*	BC022073
21	8067652	*EEF1A2*	BC110409
22	8072577	*YWHAH*	S80794
23	8072610	*FBXO7*	BC008361
24	8074856	*PRAME*	BC022008
25	8080184	*ALAS1*	AY260745
26	8080714	*FLNB*	AF043045
27	8090214	*SLC12A8|ZNF148*	AF345197
28	8090433	*MGLL*	BC006230
29	8090823	*SLCO2A1*	U70867
30	8096704	*NPNT*	AK290029
31	8110408	*THOC3|LOC728554*	BC006849
32	8110569	*SQSTM1*	BC001874
33	8114920	*DPYSL3*	BC077077
34	8115234	*ANXA6*	BC017046
35	8115886	*THOC3|LOC728554*	BC006849
36	8116780	*DSP*	M77830
37	8134869	*PCOLCE*	AB008549
38	8135990	*FLNC*	AF089841
39	8138773	*EIF4H*	BC021214
40	8143684	*PDIA4*	BC011754
41	8144669	*FDFT1*	BC009251

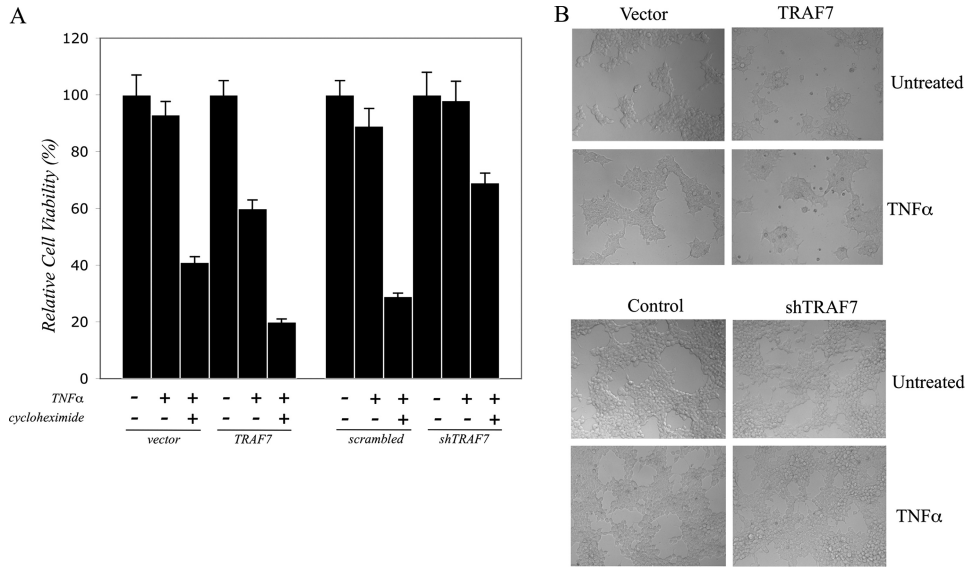

FIGURE 8. **TRAF7 promotes cell death.** *A,* HEK293 cells were transfected with the indicated expression plasmids. Twenty four hours after transfection, cell viability was determined with an MTT assay. *B,* phase contrast micrographs of HEK293 cells transfected with a vector empty or encoding for TRAF7 or with a lentiviral vector expressing a TRAF7-silencing shRNA, left untreated, or exposed for 24 h to TNFα (10 ng/ml).

TRAF7 has a negative effect on cell viability. In fact, the result of the MTT assay shown in Fig. 8*A* indicates that TRAF7 expression by itself reduces cellular viability, and in addition, it potentiates the cytotoxic effect of TNFα. Conversely, TRAF7-silenced cells exhibit higher resistance to TNFα-induced cell death. Similar results were obtained when cell viability was measured using the ATPlite assay (data not shown). Microscopy data confirmed this observation. Micrographs shown in Fig. 8*B* demonstrate that TRAF7 expression caused cellular condensation, roundup, and detachment of cells from the dish, all characteristics of apoptotic cell death.

DISCUSSION

In this study, we have identified TRAF7 as a protein that physically interacts with NEMO and with the p65 member of the NF-κB transcription factor family. This finding is consistent with the work by Bouwmeester *et al.* (3), which led to the identification of TRAF7 as a molecule participating with an interaction network of signaling proteins of the TNF receptor I. TRAF7 was also identified as a protein interacting with MEKK3 and potentiating MEKK3-induced AP-1 activation (7). The study by Bouwmeester *et al.* (3) also demonstrated that TRAF7 is an E3 ubiquitin ligase capable of self-ubiquitination. We have now identified at least two substrates, namely NEMO and p65, whose ubiquitination status is, directly or indirectly, influenced by TRAF7. It is generally accepted that nondegradative Lys-63-linked polyubiquitination of signaling molecules, including NEMO, represents a mechanism for IκB kinase recruitment and activation (4). In addition, we and others have shown that the deubiquitinating enzymes CYLD and A20 suppress NF-κB activation by targeting Lys-63-linked polyubiquitin chains on NF-κB signaling factors (13, 15–18). We now report that TRAF7 effectively promotes Lys-29-linked polyubiquitination of NEMO and p65, targeting these two proteins for lysosomal degradation. Lys-29-linked ubiquitination has been recently implicated in the regulation of AMP-activated protein kinase-related kinases. AMP-activated protein kinase family member 5 and MAPK/microtubule affinity-regulating kinase 4 are polyubiquitinated *in vivo* through Lys-29/Lys-33-coupled chains (19). This event blocks kinase activation by interfering with phosphorylation of the activation-loop residues (19). More importantly, Lys-29-linked polyubiquitin chains formed by the E3 ligase Itch/AIP4 have been implicated in lysosomal degradation of proteins (20).

Thus, in addition to the already described mechanisms (21–23), we propose that Lys-29 ubiquitination and the consequent lysosomal degradation of NEMO and p65 may represent an additional mechanism to control NF-κB activity. The experiments done using lysosomal and proteasomal inhibitors clearly support this evidence. However, as cells exposed to lysosomal inhibitors express lower levels of NEMO and p65 (Fig. 5*H*), it is possible that other proteasomal-independent mechanisms regulate NEMO and p65 protein levels.

In addition to lysosomal degradation, the TRAF7-dependent Lys-29 ubiquitination of p65 might also influence the transcriptional activity of p65. Ubiquitination has in fact emerged as a crucial mechanism that controls activity of transcription factors, including p53, c-Jun, and NF-κB (22, 24–26). Our experiments clearly show that TRAF7 induces compartmentalization of p65 into morphologically distinct structures resembling the nuclear bodies (27), and it is well known that certain nuclear bodies influence various cellular activities, including apoptosis and transcriptional regulation (28). Thus, given our results, we speculate that TRAF7 may also regulate the transcriptional activity of p65 by influencing its nuclear distribution.

Our data indicate that p65/TRAF7 interaction can take place both in the cytoplasm and in the nucleus. This is in agreement with previous works showing that TRAF7 has both a cytosolic and nuclear localization (8, 9). Thus, it is possible that the interaction in different cell compartments may have different biological implications.

The microarray analysis conducted in this work provides some valuable information on the transcriptional regulation modulated by TRAF7. Among the genes up-regulated in TRAF7-deficient cells, there are two direct targets of NF-κB, namely serpin2A (29) and matrix metallopeptidase 2 (MMP2) (30), and two genes, *IGFBP4* and *IGFBP7*, that belong to a family of proteins (31) of which two members are direct targets of NF-κB (32, 33).

However, TRAF7-deficient cells show, among others, down-regulation of the stress-related genes ceramide synthase 2 (LASS2), the ubiquitin-binding protein p62 (SQSMT1), and the apoptosis-related gene serglycin (SRGN) (34). Overall, these expression data are consistent with an inhibitory role for TRAF7 on NF-κB activation and a positive control of AP-1 transcription factor.

Clearly, our work opens many interesting questions concerning TRAF7 function that require further investigation. In this context, the generation of animal models genetically modified in the locus encoding for TRAF7 will be certainly of enormous value to finally define the physiological role of this protein.

Addendum—While this work was in preparation, Tsikitis *et al.* (35) also reported association of TRAF7 with NEMO.

Acknowledgments—We thank Drs. Simona Aufiero, Francesco Riccio, Angelica Salvatore, and Angela Zampelli for support and assistance; Drs. Laura Focareta and Carla Reale for critical reading of the manuscript; and Dr. Pietro Zoppoli and Grazia Mercadante for technical assistance in the microarray experiments. We thank Drs. C. Sasakawa and H. Ashida at University of Tokyo for kindly providing the plasmids encoding mutant ubiquitins used in this study.

REFERENCES

1. Bradley, J. R., and Pober, J. S. (2001) *Oncogene* **20,** 6482–6491
2. Wajant, H., Henkler, F., and Scheurich, P. (2001) *Cell. Signal.* **13,** 389–400
3. Bouwmeester, T., Bauch, A., Ruffner, H., Angrand, P. O., Bergamini, G., Croughton, K., Cruciat, C., Eberhard, D., Gagneur, J., Ghidelli, S., Hopf, C., Huhse, B., Mangano, R., Michon, A. M., Schirle, M., Schlegl, J., Schwab, M., Stein, M. A., Bauer, A., Casari, G., Drewes, G., Gavin, A. C., Jackson, D. B., Joberty, G., Neubauer, G., Rick, J., Kuster, B., and Superti-Furga, G. (2004) *Nat. Cell Biol.* **6,** 97–105
4. Chen, Z. J. (2005) *Nat. Cell Biol.* **7,** 758–765
5. Deng, L., Wang, C., Spencer, E., Yang, L., Braun, A., You, J., Slaughter, C., Pickart, C., and Chen, Z. J. (2000) *Cell* **103,** 351–361
6. Bianchi, K., and Meier, P. (2009) *Mol. Cell* **36,** 736–742
7. Xu, L. G., Li, L. Y., and Shu, H. B. (2004) *J. Biol. Chem.* **279,** 17278–17282
8. Morita, Y., Kanei-Ishii, C., Nomura, T., and Ishii, S. (2005) *Mol. Biol. Cell* **16,** 5433–5444
9. Yoshida, H., Jono, H., Kai, H., and Li, J. D. (2005) *J. Biol. Chem.* **280,** 41111–41121
10. Ghosh, S., May, M. J., and Kopp, E. B. (1998) *Annu. Rev. Immunol.* **16,** 225–260
11. Silverman, N., and Maniatis, T. (2001) *Genes Dev.* **15,** 2321–2342
12. Stilo, R., Leonardi, A., Formisano, L., Di Jeso, B., Vito, P., and Liguoro, D. (2002) *FEBS Lett.* **521,** 165–169
13. Stilo, R., Varricchio, E., Liguoro, D., Leonardi, A., and Vito, P. (2008) *J. Cell Sci.* **121,** 1165–1171
14. Gao, Z., Chiao, P., Zhang, X., Zhang, X., Lazar, M. A., Seto, E., Young, H. A., and Ye, J. (2005) *J. Biol. Chem.* **280,** 21091–21098
15. Brummelkamp, T. R., Nijman, S. M., Dirac, A. M., and Bernards, R. (2003) *Nature* **424,** 797–801
16. Kovalenko, A., Chable-Bessia, C., Cantarella, G., Israël, A., Wallach, D., and Courtois, G. (2003) *Nature* **424,** 801–805
17. Boone, D. L., Turer, E. E., Lee, E. G., Ahmad, R. C., Wheeler, M. T., Tsui, C., Hurley, P., Chien, M., Chai, S., Hitotsumatsu, O., McNally, E., Pickart, C., and Ma, A. (2004) *Nat. Immunol.* **5,** 1052–1060
18. Wertz, I. E., O'Rourke, K. M., Zhou, H., Eby, M., Aravind, L., Seshagiri, S., Wu, P., Wiesmann, C., Baker, R., Boone, D. L., Ma, A., Koonin, E. V., and Dixit, V. M. (2004) *Nature* **430,** 694–699
19. Al-Hakim, A. K., Zagorska, A., Chapman, L., Deak, M., Peggie, M., and Alessi, D. R. (2008) *Biochem. J.* **411,** 249–260
20. Chastagner, P., Israël, A., and Brou, C. (2006) *EMBO Rep.* **7,** 1147–1153
21. Beg, A. A., Sha, W. C., Bronson, R. T., and Baltimore, D. (1995) *Genes Dev.* **9,** 2736–2746
22. Saccani, S., Marazzi, I., Beg, A. A., and Natoli, G. (2004) *J. Exp. Med.* **200,** 107–113
23. Geng, H., Wittwer, T., Dittrich-Breiholz, O., Kracht, M., and Schmitz, M. L. (2009) *EMBO Rep.* **10,** 381–386
24. Dornan, D., Wertz, I., Shimizu, H., Arnott, D., Frantz, G. D., Dowd, P., O'Rourke, K., Koeppen, H., and Dixit, V. M. (2004) *Nature* **429,** 86–92
25. Tanaka, T., Grusby, M. J., and Kaisho, T. (2007) *Nat. Immunol.* **8,** 584–591
26. Ryo, A., Suizu, F., Yoshida, Y., Perrem, K., Liou, Y. C., Wulf, G., Rottapel, R., Yamaoka, S., and Lu, K. P. (2003) *Mol. Cell* **12,** 1413–1426
27. Zimber, A., Nguyen, Q. D., and Gespach, C. (2004) *Cell. Signal.* **16,** 1085–1104
28. Zhong, S., Salomoni, P., and Pandolfi, P. P. (2000) *Nat Cell Biol.* **2,** E85–E90
29. Hampson, L., Hampson, I. N., Babichuk, C. K., Cotter, L., Bleackley, R. C., Dexter, T. M., and Cross, M. A. (2001) *Hematol. J.* **2,** 150–160
30. Liu, L. P., Liang, H. F., Chen, X. P., Zhang, W. G., Yang, S. L., Xu, T., and Ren, L. (2010) *Cancer Invest.* **28,** 443–451
31. Ruan, W., and Lai, M. (2010) *Acta Diabetol.* **47,** 5–14
32. Cazals, V., Nabeyrat, E., Corroyer, S., de Keyzer, Y., and Clement, A. (1999) *Biochim. Biophys. Acta* **1448,** 349–362
33. Lang, C. H., Nystrom, G. J., and Frost, R. A. (1999) *Am. J. Physiol.* **276,** G719–G727
34. Metkar, S. S., Wang, B., Aguilar-Santelises, M., Raja, S. M., Uhlin-Hansen, L., Podack, E., Trapani, J. A., and Froelich, C. J. (2002) *Immunity* **16,** 417–428
35. Tsikitis, M., Acosta-Alvear, D., Blais, A., Campos, E. I., Lane, W. S., Sánchez, I., and Dynlacht, B. D. (2010) *EMBO Rep.* **11,** 969–976